

- Various Displacement Well Response Testing - A Well Performance Testing Methodology to Identify Nonlinear Formation-Controlled Flow

M.A. Zenner
- Free University of Berlin -

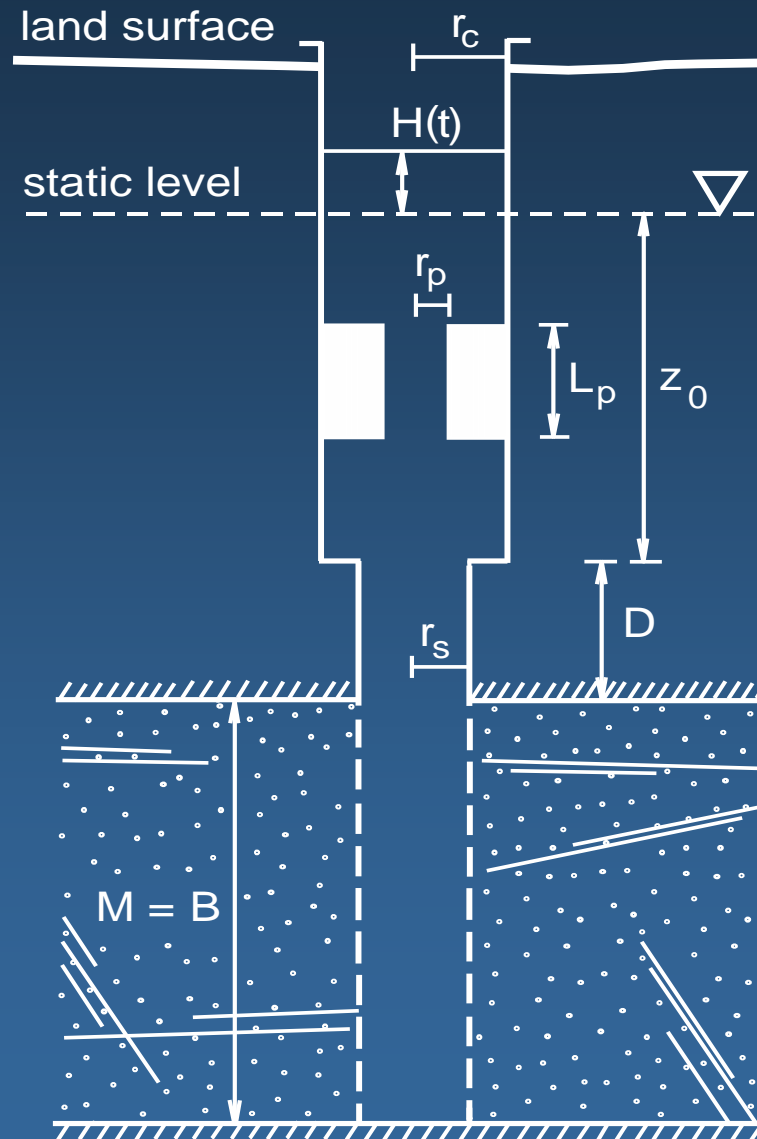
presented at the PetroTherm-Seminar of the
Karlsruhe Institute of Technology (KIT), Karlsruhe, December 15, 2011

- Motivation – Why well testing?
 - Status Quo – Classical linear slug test theories
 - Observed anomalies
 - A new fully nonlinear slug test model
 - Applications of the new nonlinear slug test model
 - Perspectives – Testing of low-permeability formations
 - Summary
-

Why well testing?

- **Well testing can identify reservoir complexity** (e.g. reservoir boundaries)! Reservoir complexity usually is unknown in the early stage of an investigation but knowledge of reservoir complexity is needed to render numerical reservoir simulation meaningful.
- **Well testing directly provides „upscaled“ hydraulic parameters** (needed for numerical flow simulation).
- **Well testing allows to identify reservoir leakage** (important to determine reservoir/aquifer integrity).
- **Well testing provides well productivities/injectivities** (important to determine the economical feasibility of geothermal/hydrocarbon exploitation and sub-surface storage projects).
- **This presentation shows: Various displacement well response testing allows to identify nonlinear formation-controlled flow.**
 - > supports an identification of hydraulically conductive fractures
 - > relevant to cap rock tightness characterization
 - > relevant to fractured/karstified reservoir characterization

Status Quo - Classical linear slug test theories



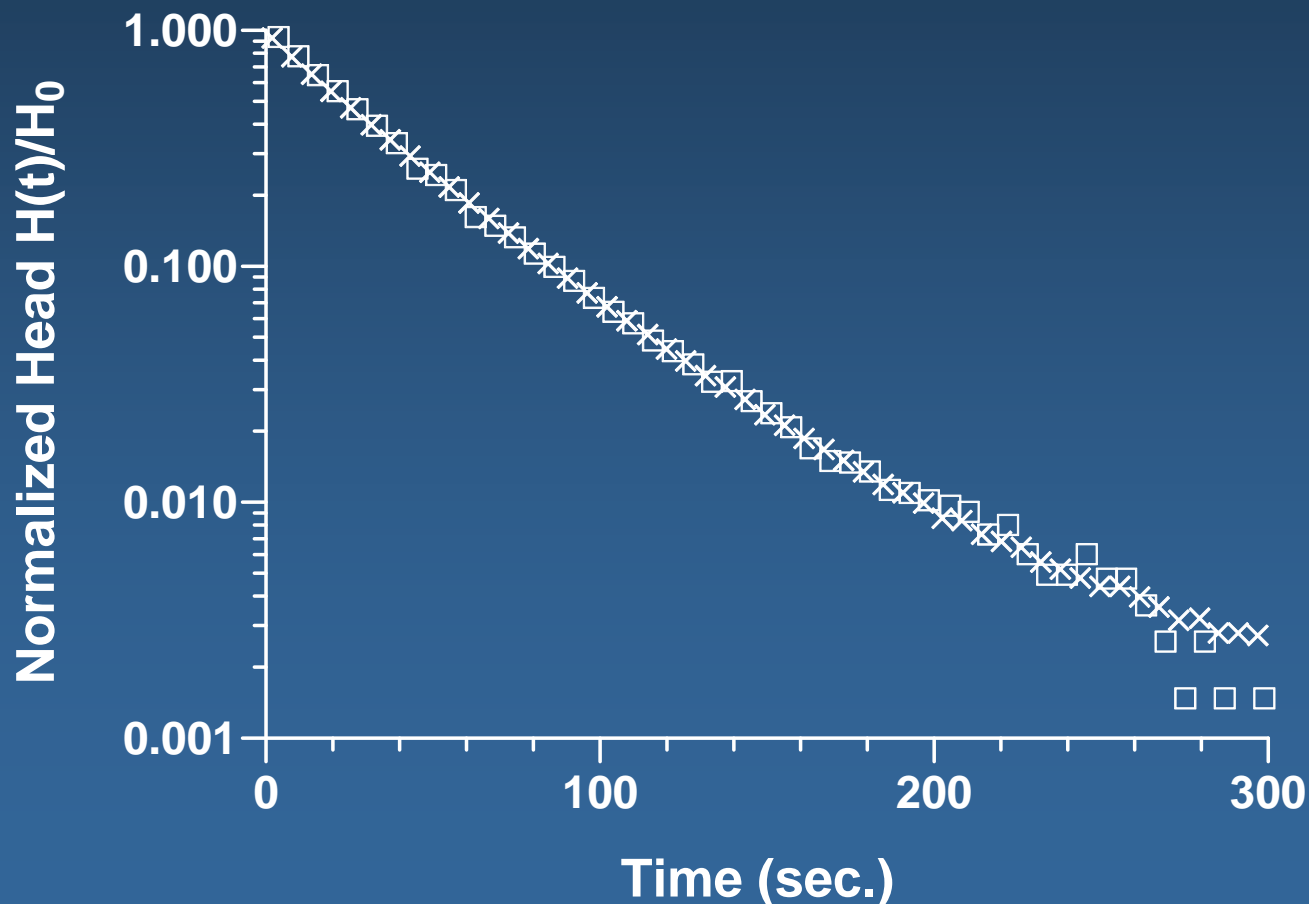
Cooper-Bredehoeft-Papadopoulos (CBP) Model (1967):

$$\frac{H(t)}{H_0} = \frac{8r_s^2 S}{\pi^2 r_c^2} \cdot \int_0^{\infty} \frac{1}{u \cdot \Delta u} \exp\left\{-\frac{Ttu^2}{r_s^2 S}\right\} du$$

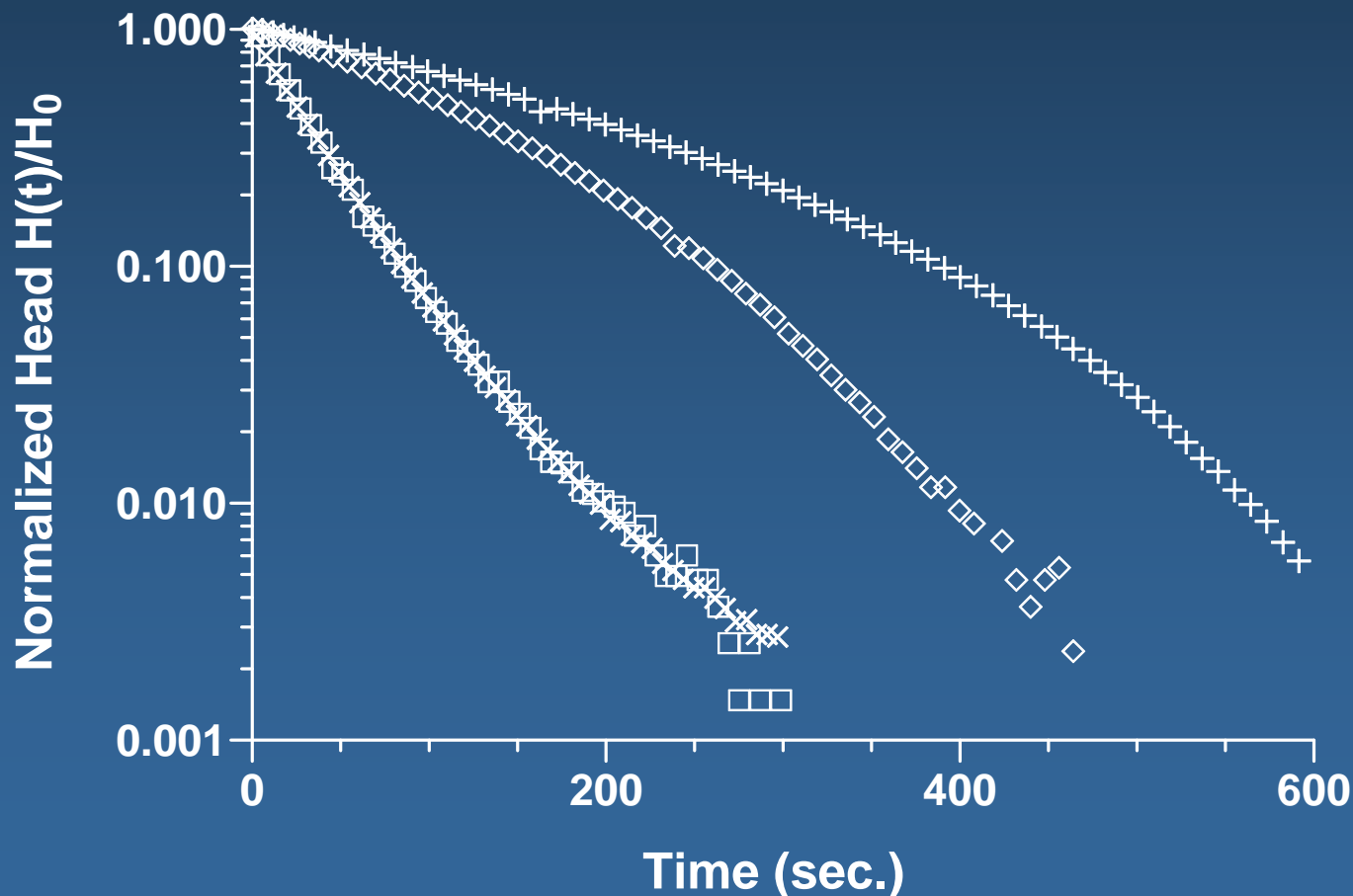


The right-hand side is independent of H_0 !

Classical normalized head responses are convex or linear collapsing onto a unique curve for different H_0 :



The Problem: We have observed concave normalized head responses not collapsing onto a unique curve:



Fully nonlinear slug test model for finite diameter wells
(Zenner, 2008, 2009):

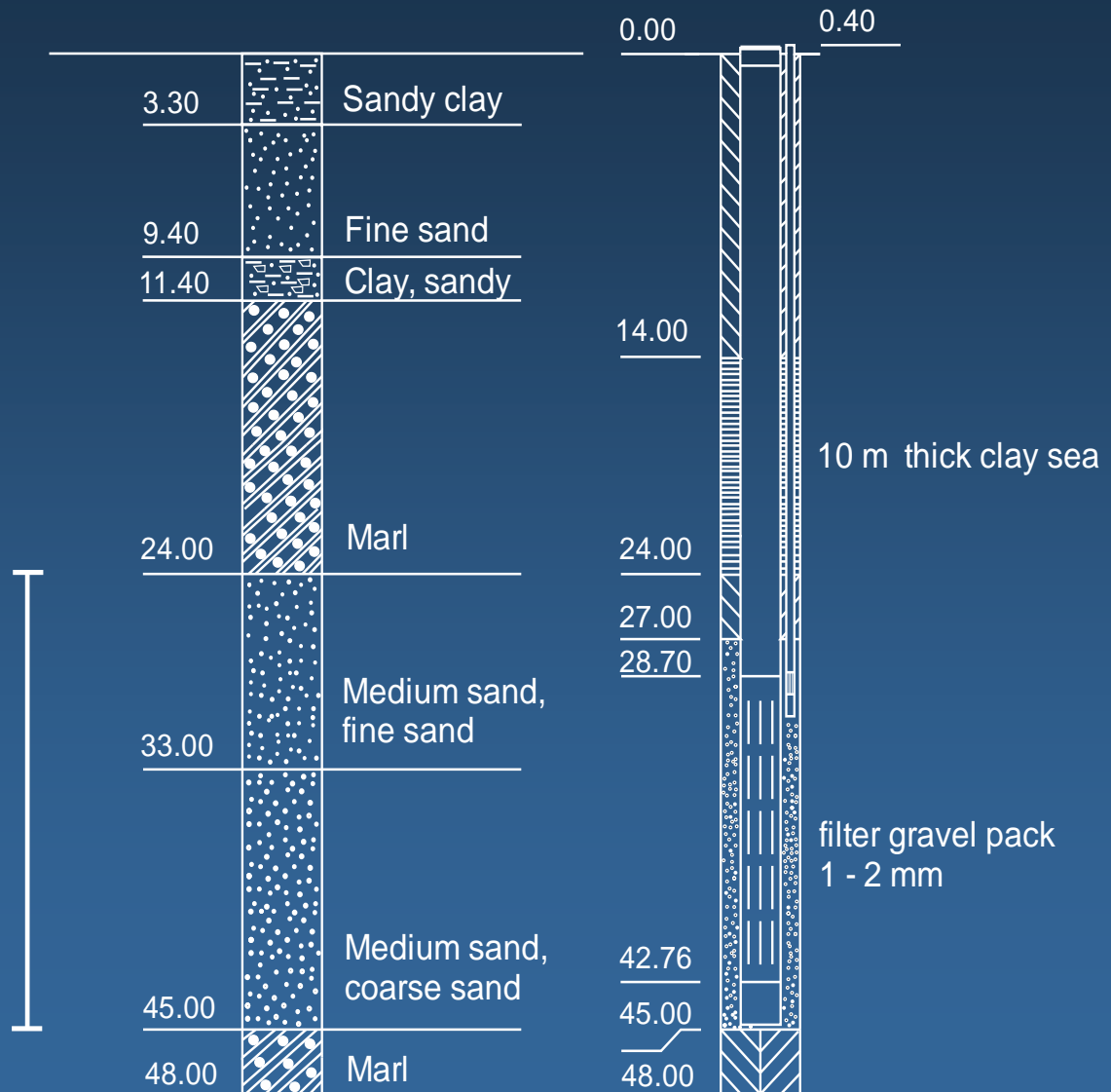
$$\begin{aligned}
 & - \left(H + z_0 + \left[\frac{r_c^2}{r_p^2} - 1 \right] L_p + \left[\frac{3}{8} B + D \right] \frac{r_c^2}{r_s^2} \right) \frac{d^2 H}{dt^2} - gH \\
 & + \frac{1}{2} \left[\left(\frac{r_c^2}{2r_s B} \right)^2 - 1 + \xi_{\text{loss}} - \left(f_p \frac{L_p r_c^4}{2r_p^5} + f_s \frac{D r_c^4}{2r_s^5} + f_c \frac{z_0 - L_p + H}{2r_c} \right) \text{sign} \left(\frac{dH}{dt} \right) \right] \left(\frac{dH}{dt} \right)^2 \\
 & - g \pi r_c^2 \left(B_2 + C (\pi r_c^2)^{p-1} \left| \frac{dH}{dt} \right|^{p-1} \right) \frac{dH}{dt} - \frac{g r_c^2}{2 \pi^2 T} \int_0^t \frac{\partial^2 H}{\partial \tau^2} \int_0^\infty \frac{1 - e^{-\frac{4T(t-\tau)x^2}{S r_D^2}}}{x^3 [J_1^2(2x) + Y_1^2(2x)]} dx d\tau = 0
 \end{aligned}$$

Applications of the new nonlinear slug test model

Example No. 1:

Slug test analysis at well
B-7004 (Berlin,
Tempelhof Airport)

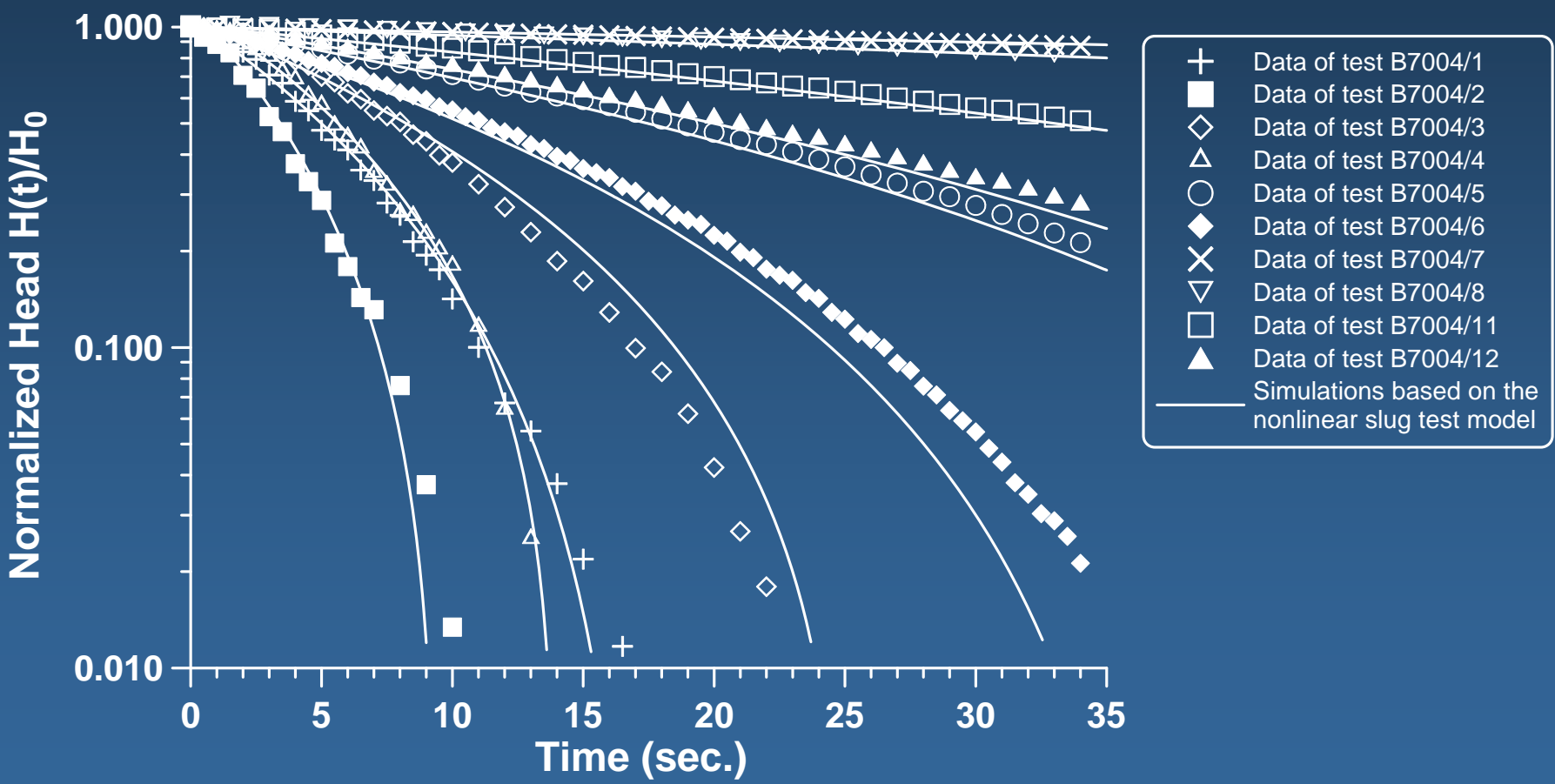
Aquifer thickness



Test design to investigate packer-related nonlinear head loss components:

Slug Test Identifier	r_p (m)	L_p (m)	H_0 (m)
B7004/1	0.025	1.774	3.96
B7004/2	0.025	1.774	1.35
B7004/3	0.025	9.774	4.15
B7004/4	0.025	9.774	1.35
B7004/5	0.014	1.774	4.12
B7004/6	0.014	1.774	1.33
B7004/7	0.0055	1.774	4.09
B7004/8	0.0055	1.774	1.33
B7004/11	0.014	9.774	4.21
B7004/12	0.014	9.774	1.36

Measured vs. simulated responses at well B-7004:



Inferences from Example No. 1:

- Nonlinear tubing-controlled flow causes concavity and implies a shift of normalized head responses toward larger times.
- Colebrook and Borda Carnot-type head loss formulas from steady state pipe hydraulics are sufficiently accurate at modeling tubing-controlled transient flow inside the well.

Example No. 2:

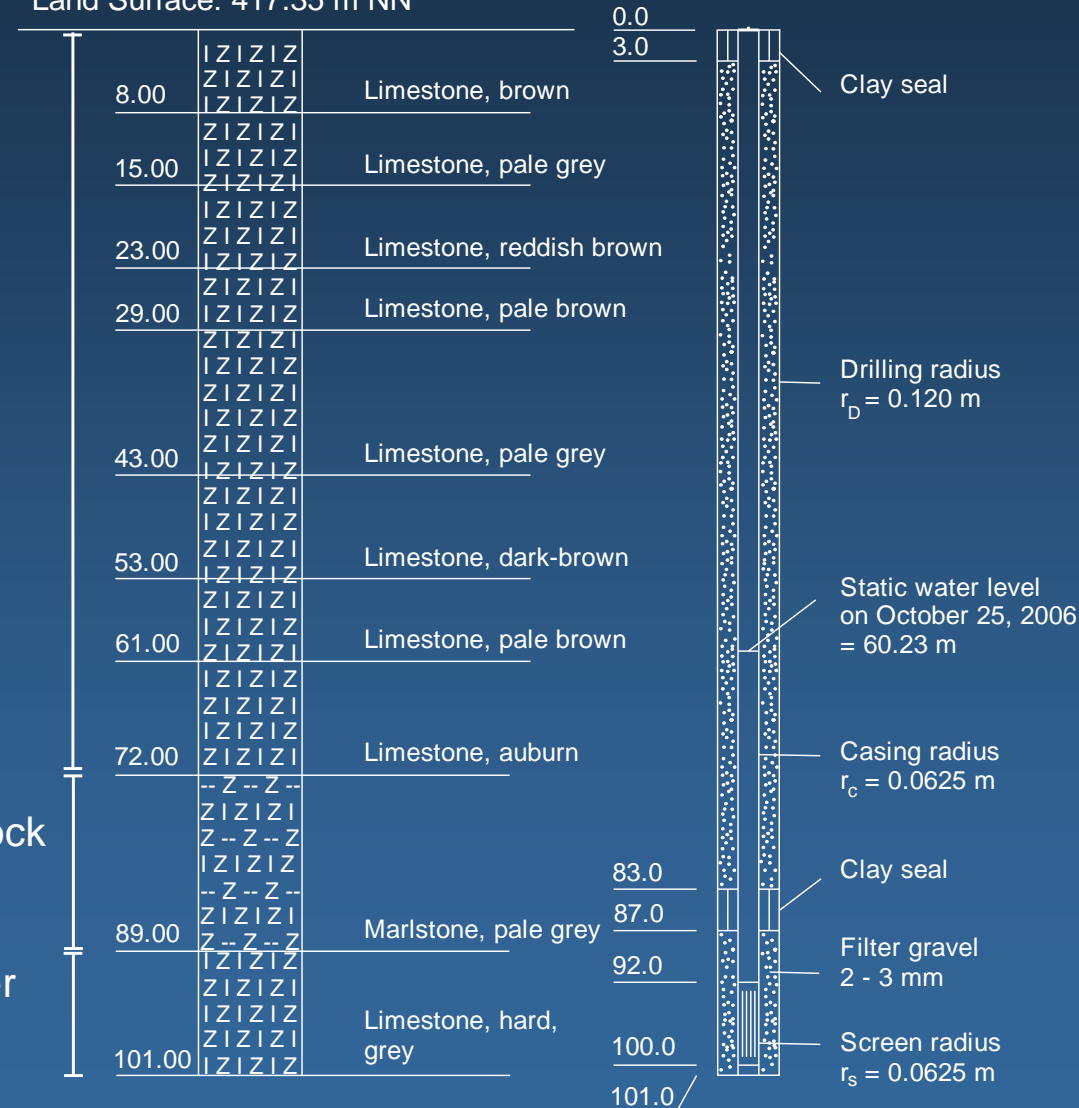
Slug test analysis at well Münstereifelbohrung B2 (Eifel-Area)

Overburden

Confining cap-rock
layer

Fractured aquifer
thickness

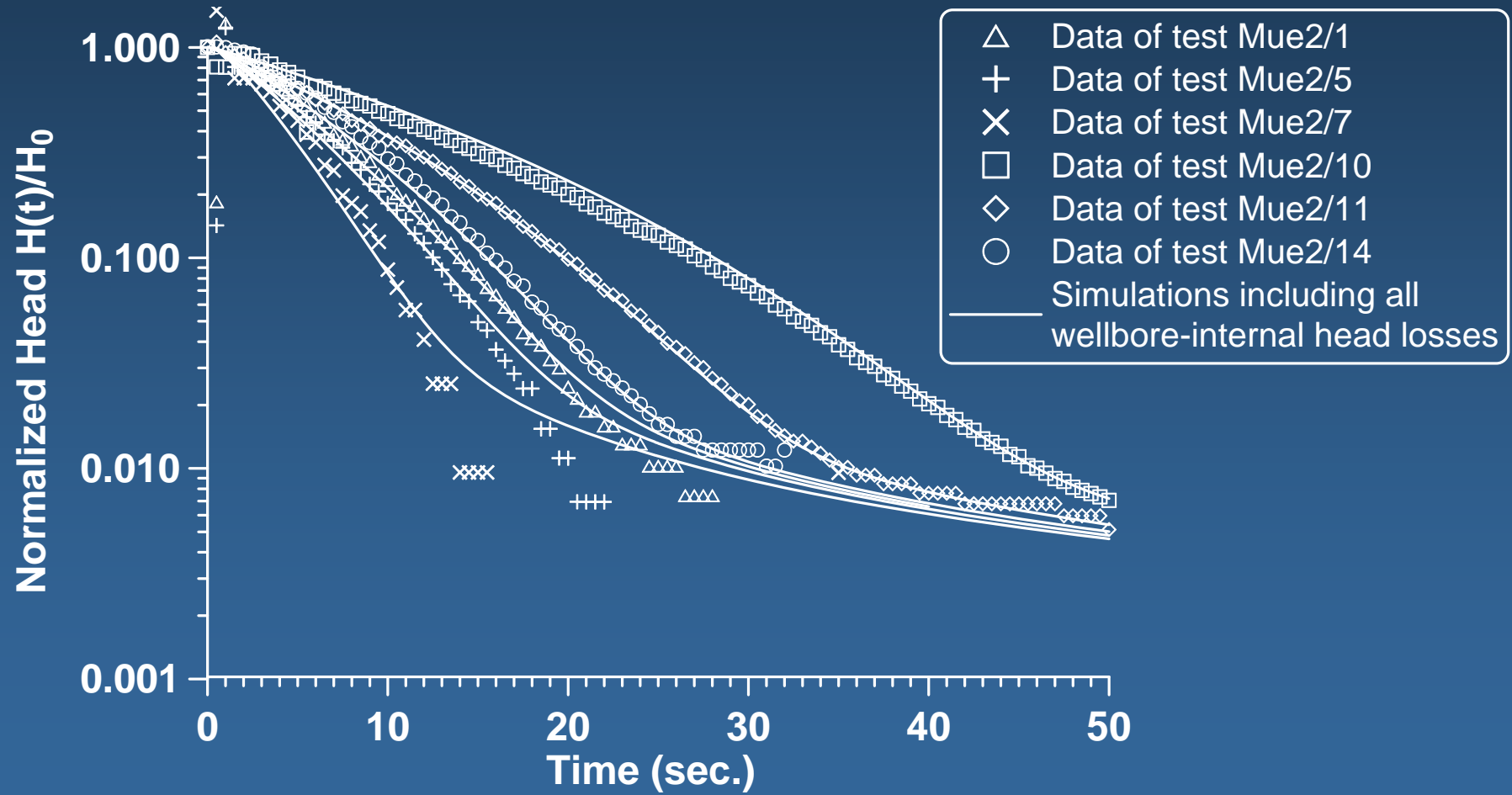
Land Surface: 417.35 m NN



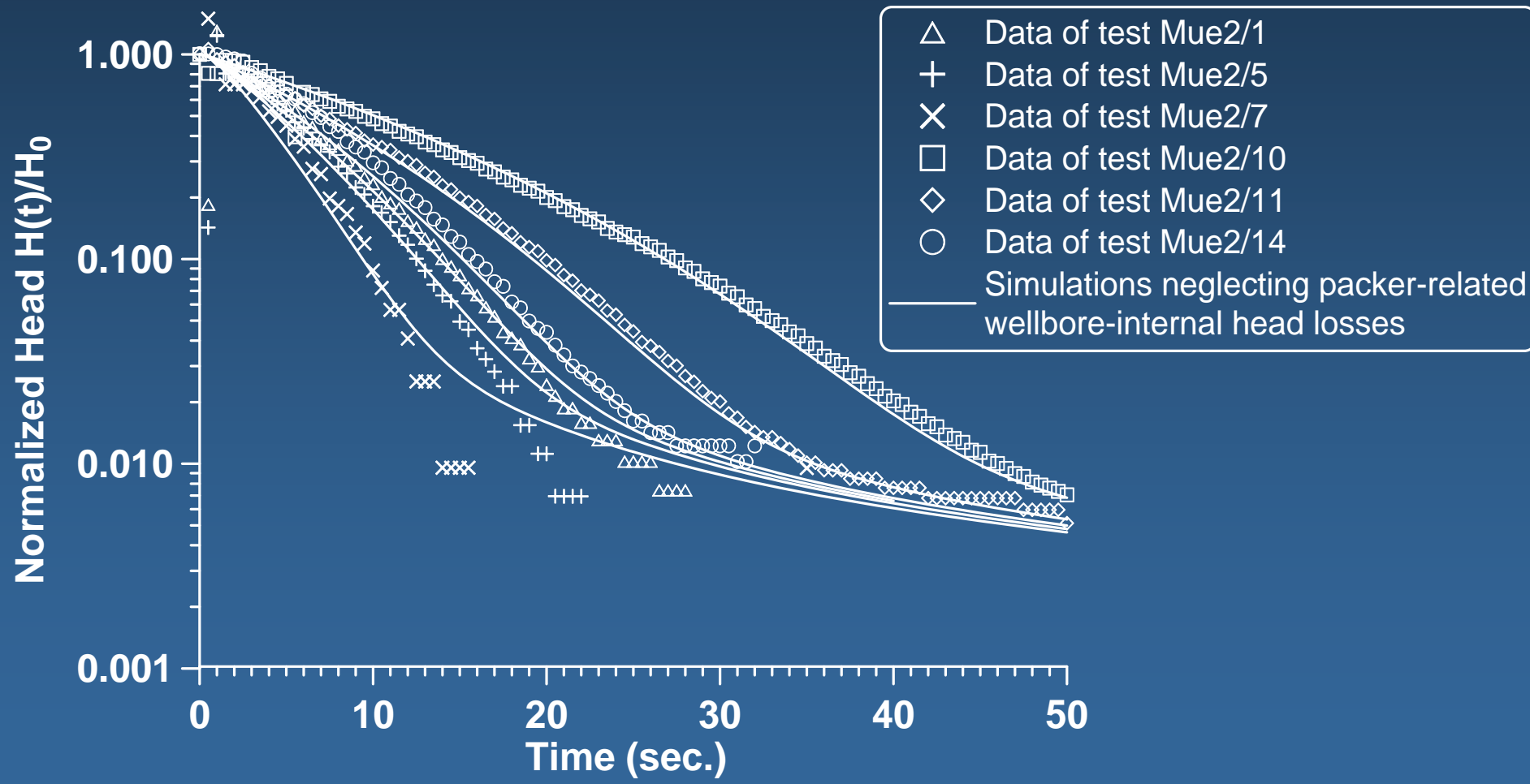
Test design to investigate the flow dynamics inside the fractured Devonian limestone formation:

Slug Test Identifier	r_p (m)	L_p (m)	C (s^p/m^{3p-1})	p (-)	H_0 (m)
Mue2/1	0.0625	0	23500	1.6	- 0.715
Mue2/5	0.0625	0	23500	1.6	- 0.475
Mue2/7	0.0625	0	23500	1.6	- 0.129
Mue2/10	0.0250	1.774	23500	1.6	+7.470
Mue2/11	0.0250	1.774	23500	1.6	+2.420
Mue2/14	0.0250	1.774	23500	1.6	+1.020

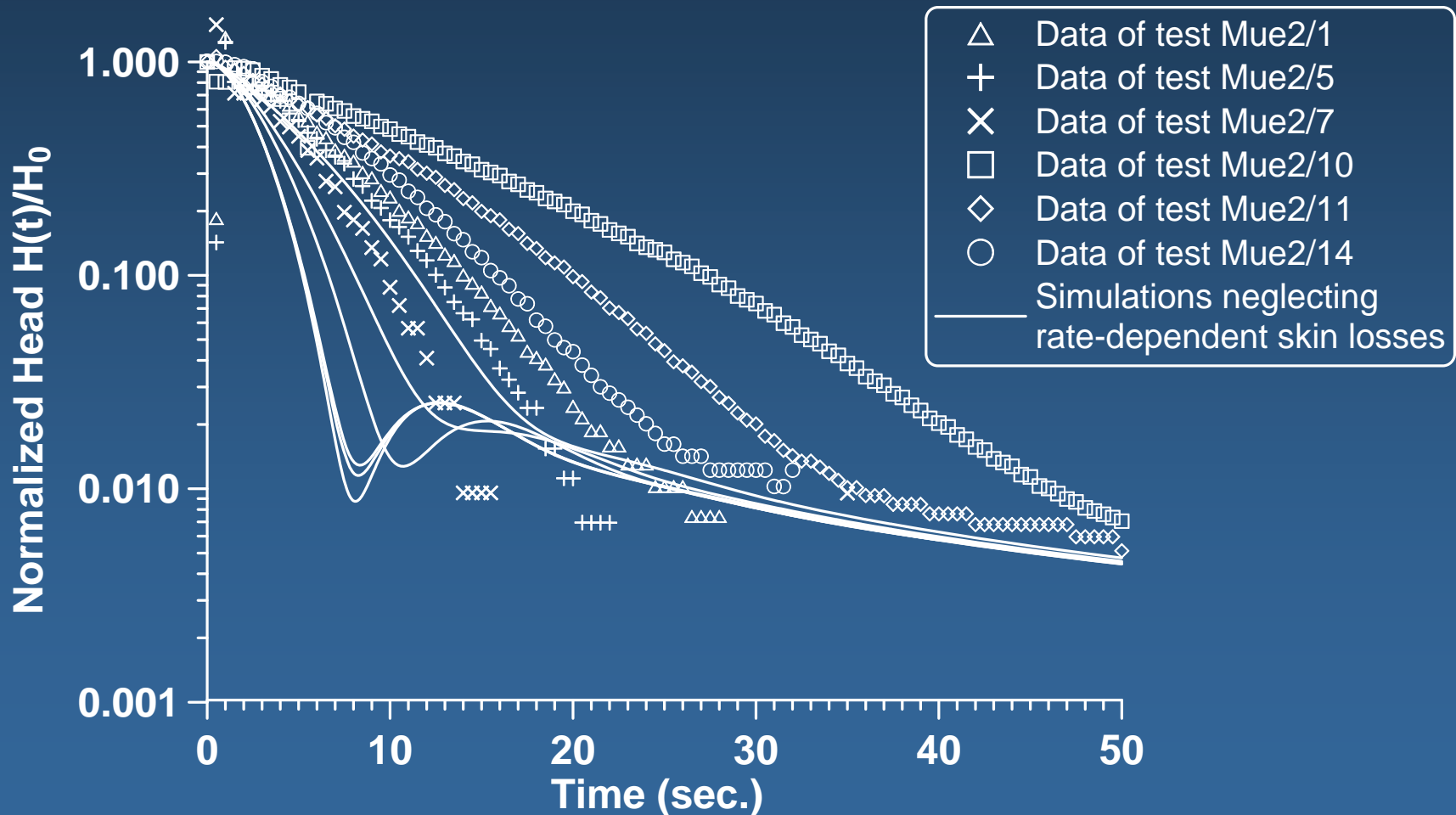
Measured vs. simulated responses at well Münstereifelbohrung B2:



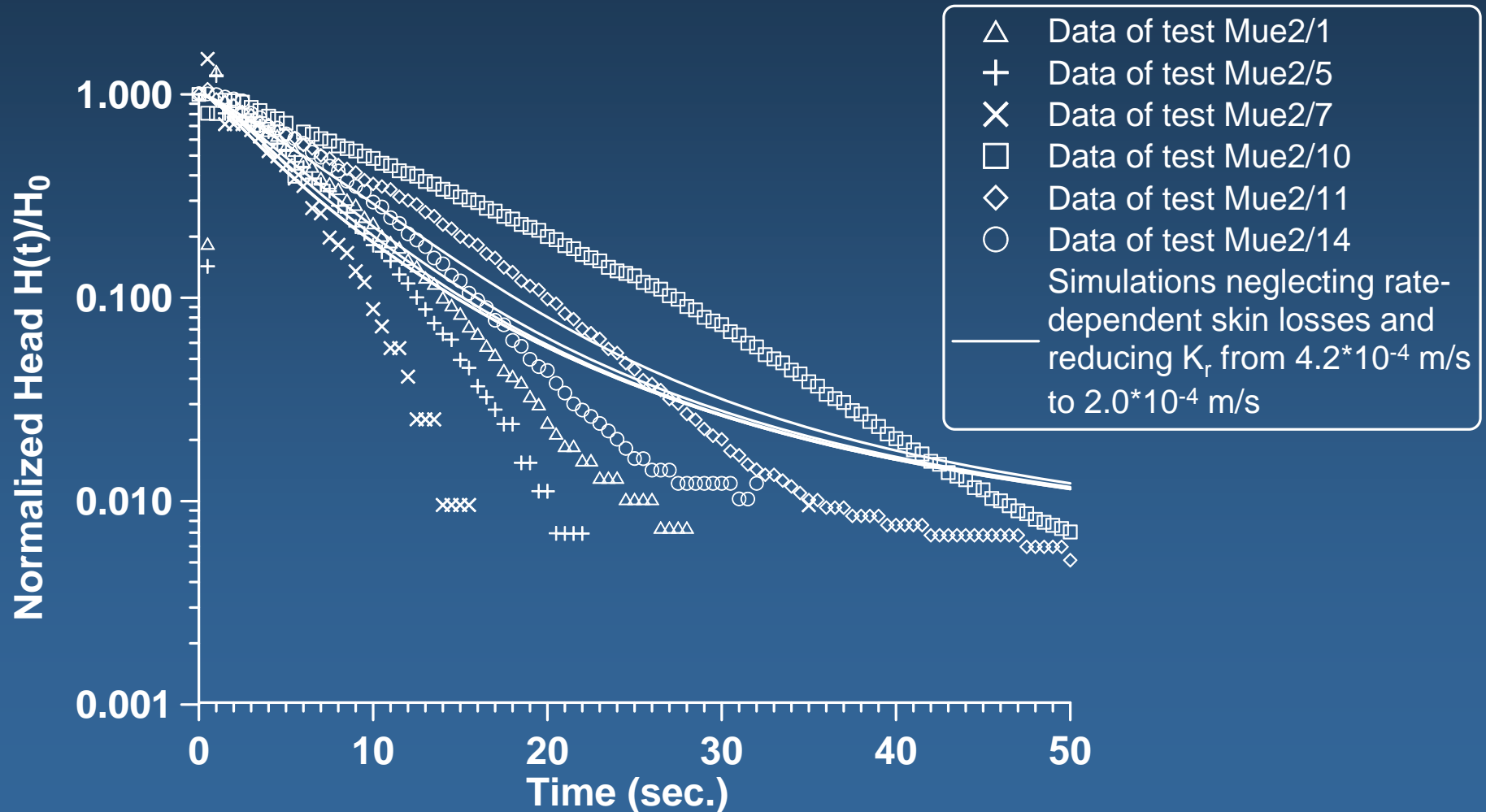
Measured vs. simulated responses at well Münstereifelbohrung B2:



Measured vs. simulated responses at well Münstereifelbohrung B2:



Measured vs. simulated responses at well Münstereifelbohrung B2:



Inferences from Example No. 2:

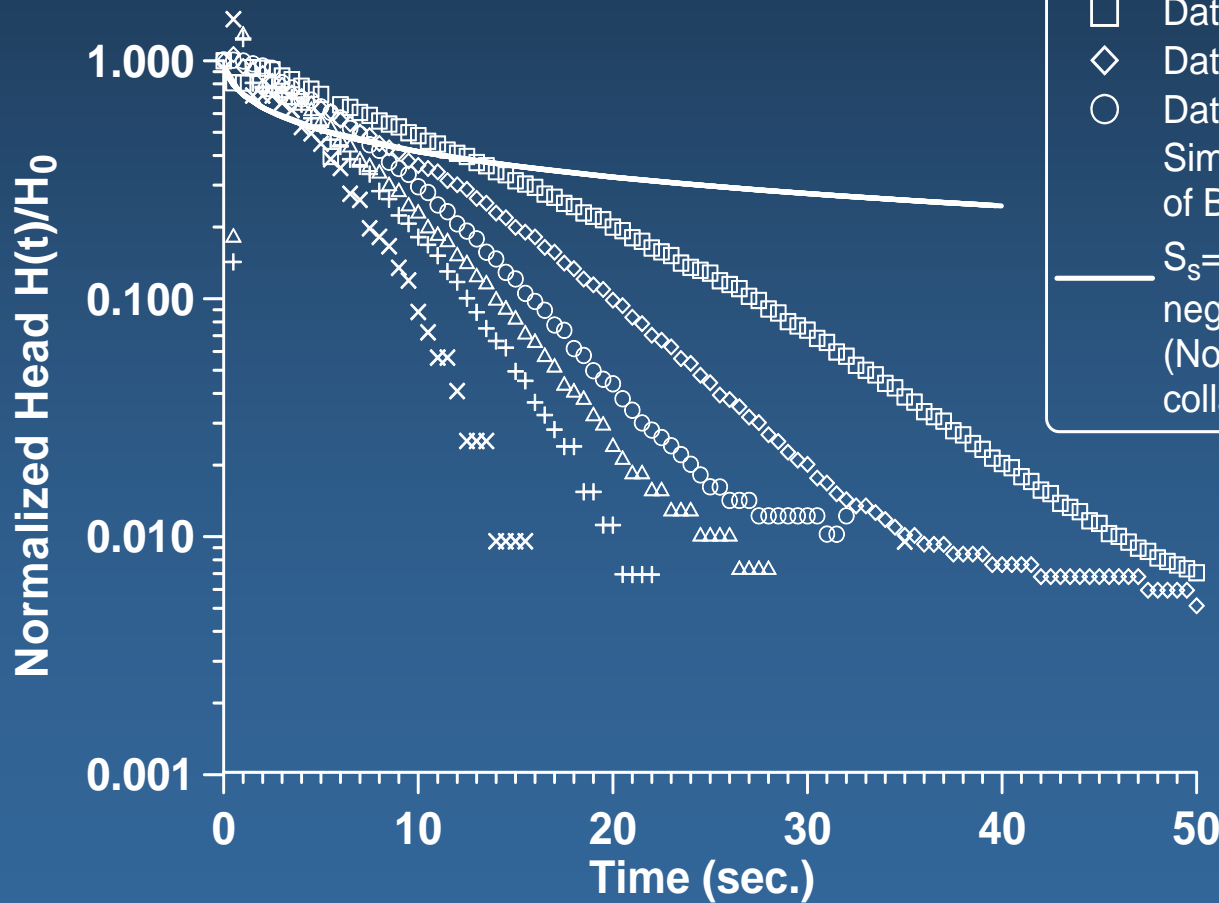
- Nonlinear formation-controlled flow causes concavity and implies a shift of normalized head responses toward larger times similar to tubing-controlled flow.
 - A differentiation of formation-controlled and tubing-controlled flow is possible but requires detailed knowledge of the geometric configurations of fittings (e.g. a packer) used inside the wellbore.
 - Particularly, various-displacement well response testing can identify near-well nonlinear flow in fractured/karstified rock!
- > *Combine it with production logging or high-resolution borehole imaging techniques like FMI, UBI, AT to maximize structural and hydraulic information on investigated fractured systems.*

Example No. 3 (a theoretical consideration):

Can fractional flow account for the observed head responses? Consider the fractional flow model of Barker (1988):

$$S_s \frac{\partial s}{\partial t} = \frac{k}{r^{n-1}} \cdot \frac{\partial}{\partial r} \left(r^{n-1} \frac{\partial s}{\partial r} \right)$$

Applications of the new nonlinear slug test model



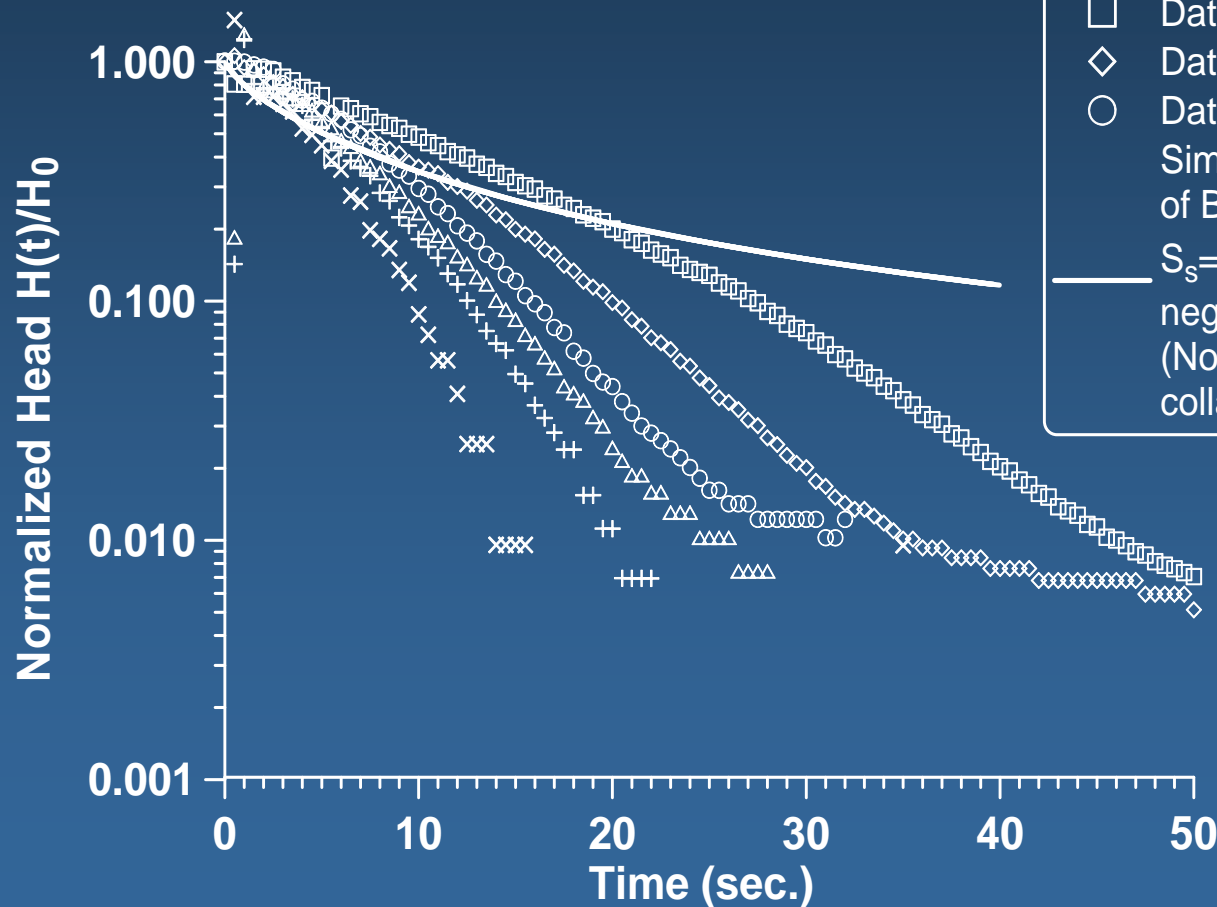
- \triangle Data of test Mue2/1
- $+$ Data of test Mue2/5
- \times Data of test Mue2/7
- \square Data of test Mue2/10
- \diamond Data of test Mue2/11
- \circ Data of test Mue2/14

Simulations: Linear fractional flow model of Barker (1988) ($n=1.0$, $k=2.0 \cdot 10^{-4}$ m/s, $S_s=1.0 \cdot 10^{-6}$ m $^{-1}$, all nonlinear head losses neglected)

(Note: Simulated responses exactly collapse onto a unique convex curve)

Simulations performed as "pulsed" production/injection tests for a pumping/injection period of $\Delta t=0.1$ sec. and corresponding rates:
 $Q_{\text{pump}} = -\pi r_c r_c H_0 / \Delta t$ m 3 /sec.

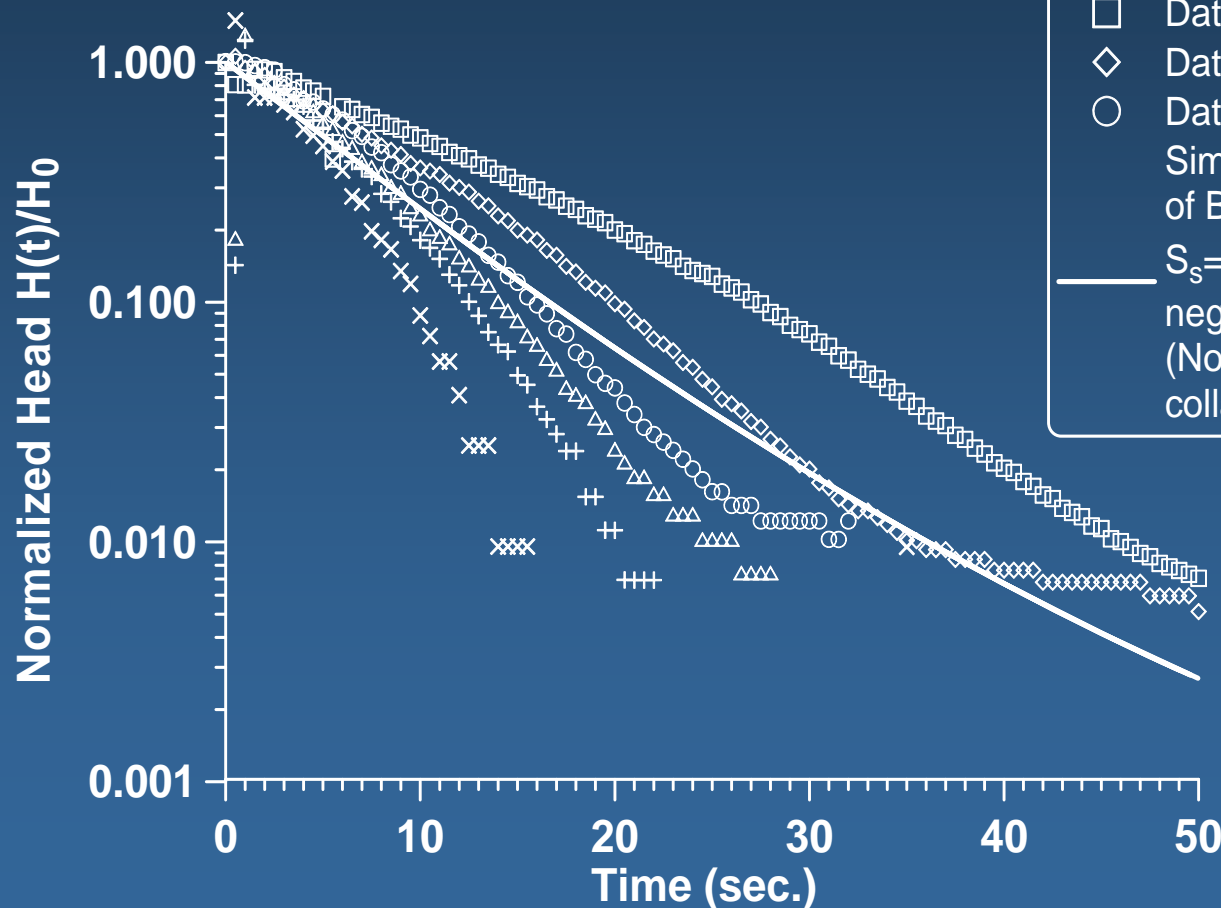
Applications of the new nonlinear slug test model



\triangle Data of test Mue2/1
 $+$ Data of test Mue2/5
 \times Data of test Mue2/7
 \square Data of test Mue2/10
 \diamond Data of test Mue2/11
 \circ Data of test Mue2/14
 Simulations: Linear fractional flow model of Barker (1988) ($n=1.5$, $k=1.0 \cdot 10^{-4}$ m/s, $S_s=1.0 \cdot 10^{-6}$ m $^{-1}$, all nonlinear head losses neglected)
 (Note: Simulated responses exactly collapse onto a unique convex curve)

Simulations performed as "pulsed" production/injection tests for a pumping/injection period of $\Delta t=0.1$ sec. and corresponding rates:
 $Q_{\text{pump}} = -\pi r_c r_c H_0 / \Delta t$ m 3 /sec.

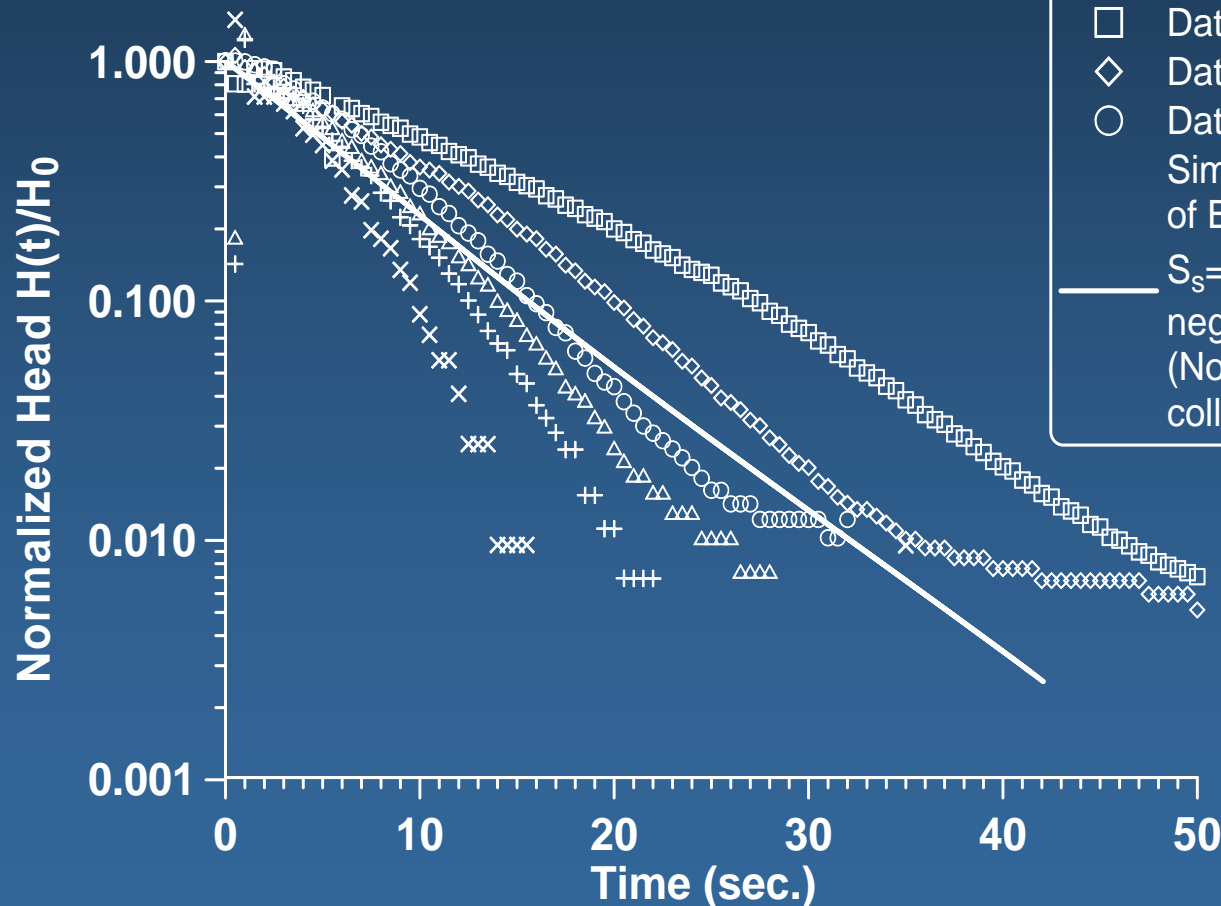
Applications of the new nonlinear slug test model



\triangle Data of test Mue2/1
 $+$ Data of test Mue2/5
 \times Data of test Mue2/7
 \square Data of test Mue2/10
 \diamond Data of test Mue2/11
 \circ Data of test Mue2/14
 Simulations: Linear fractional flow model of Barker (1988) ($n=2.5$, $k=3.0 \cdot 10^{-4}$ m/s, $S_s=1.0 \cdot 10^{-6}$ m $^{-1}$, all nonlinear head losses neglected)
 (Note: Simulated responses exactly collapse onto a unique convex curve)

Simulations performed as "pulsed" production/injection tests for a pumping/injection period of $\Delta t=0.1$ sec. and corresponding rates:
 $Q_{\text{pump}} = -\pi r_c r_c H_0 / \Delta t$ m 3 /sec.

Applications of the new nonlinear slug test model



△ Data of test Mue2/1
 + Data of test Mue2/5
 × Data of test Mue2/7
 □ Data of test Mue2/10
 ◇ Data of test Mue2/11
 ○ Data of test Mue2/14
 Simulations: Linear fractional flow model of Barker (1988) ($n=3.0$, $k=1.2 \cdot 10^{-3}$ m/s, $S_s=1.0 \cdot 10^{-6}$ m⁻¹, all nonlinear head losses neglected)
 (Note: Simulated responses exactly collapse onto a unique linear curve)

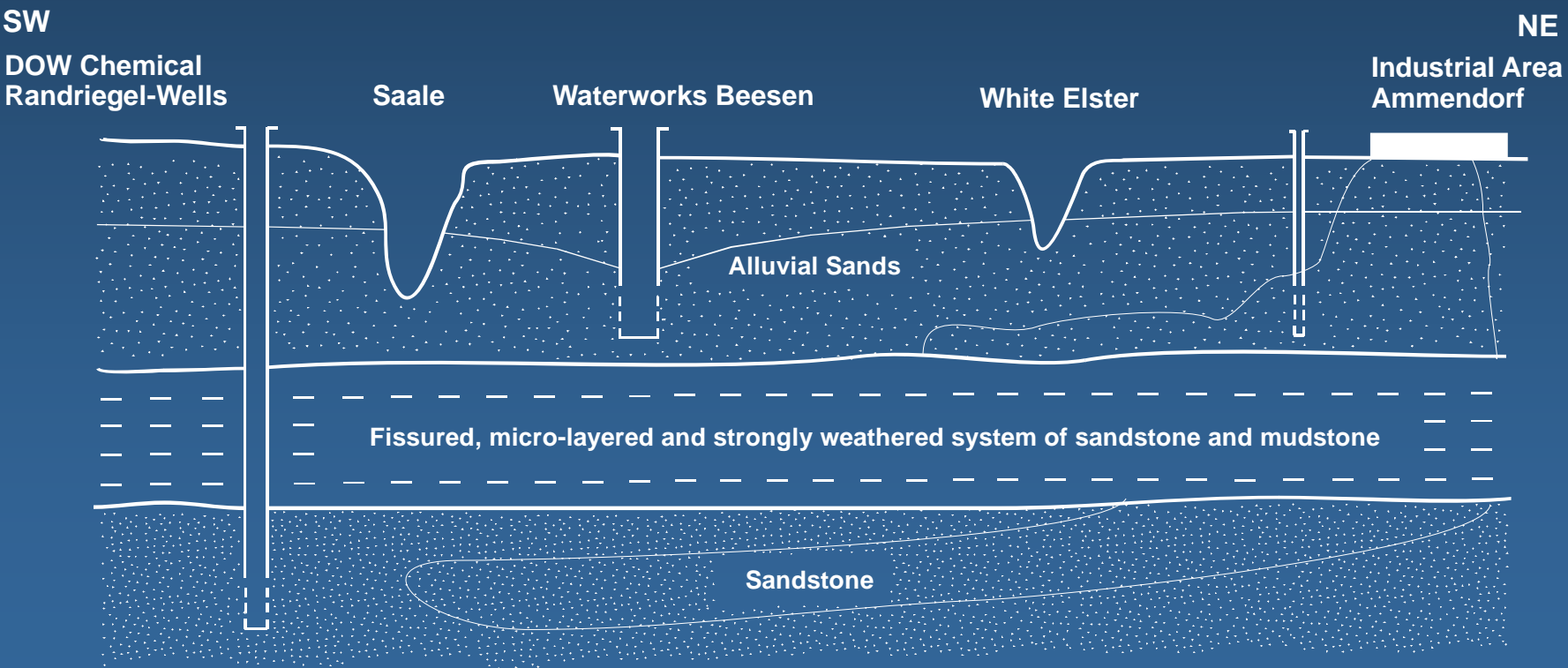
Simulations performed as "pulsed" production/injection tests for a pumping/injection period of $\Delta t=0.1$ sec. and corresponding rates:
 $Q_{\text{pump}} = -\pi r_c r_c H_0 / \Delta t$ m³/sec.

Inferences from Example No. 3:

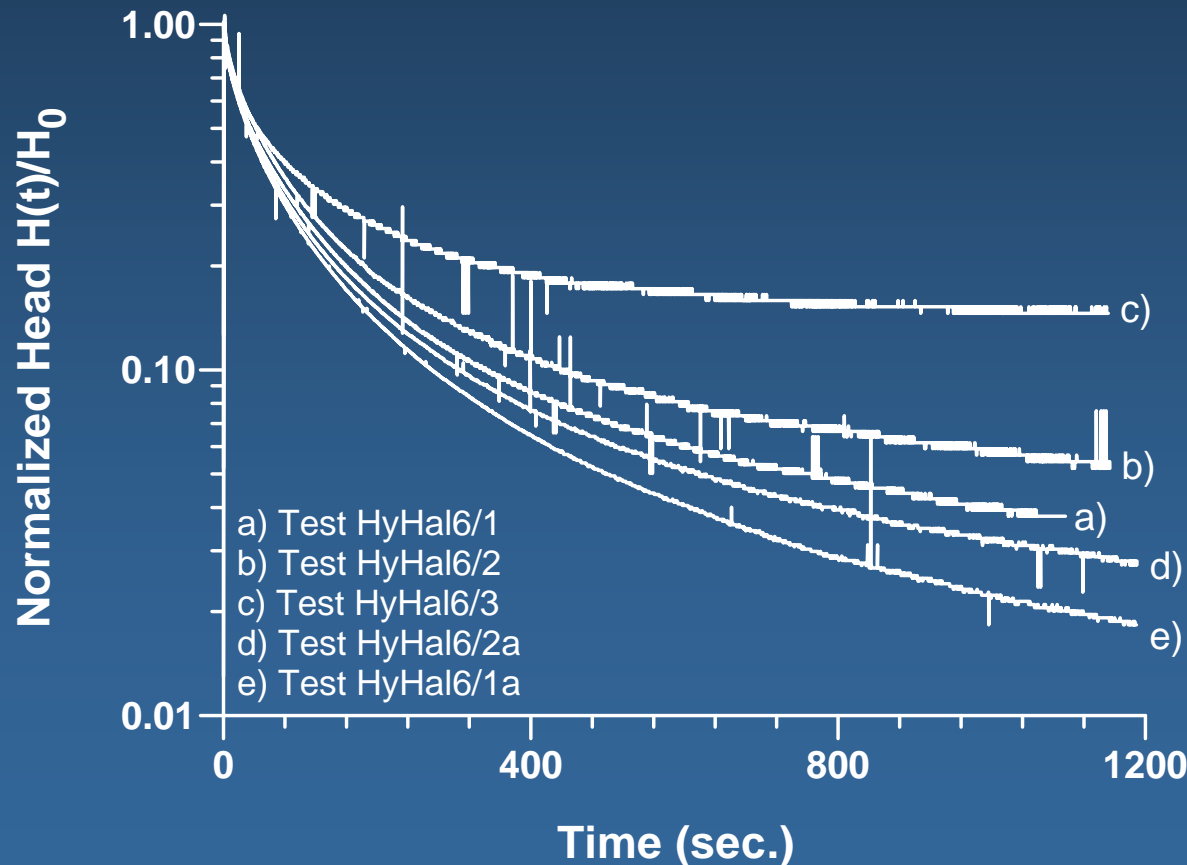
- Fractional flow does NOT provide concave normalized head responses in a Hvorslev-style format.
- Fractional flow does NOT yield shifted-in-time normalized head responses when using differing initial displacements H_0 .
- Consequently, fractional flow is NOT the physical process causing the head responses observed at well Münstereifelbohrung B2.

Waterworks Beesen at Halle, Saxony-Anhalt

An example of characterizing a hydraulic barrier



Head responses are convex and reproducible for the weathered sandstone/mudstone unit; however, responses do not collapse onto a unique curve for different H_0 . This may potentially be due to pseudo-plastic flow.



Summary

- Nonlinearity is evident from well response testing either by concave or by convex normalized head response curves, which are significantly shifted against one another when using varying displacements H_0 . Fractional flow does not imply this head-dependent behavior.
- Nonlinear formation-controlled flow characteristics cannot be inferred from core analyses (poro-perm data) but may inexpensively be estimated by various displacement well response testing.
- Various displacement well response testing may especially be promising at:
 - *hydraulic characterizations of fractured and karstified formations envisioned for drinking water supply and geothermal energy exploitation,*
 - *tightness characterization of fractured reservoir cap rocks and hydraulic barriers,*
 - *and potentially also for nuclear waste repository analyses.*

--- Backup ---

Mechanical energy balance of the water inside the wellbore:

$$\begin{aligned}
 & - \left(H + z_0 + \left[\frac{r_c^2}{r_p^2} - 1 \right] L_p + \left[\frac{3}{8} B + D \right] \frac{r_c^2}{r_s^2} \right) \frac{d^2 H}{dt^2} - g \pi r_c^2 \left(B_2 + C (\pi r_c^2)^{p-1} \left| \frac{dH}{dt} \right|^{p-1} \right) \frac{dH}{dt} \\
 & + \frac{1}{2} \left[\left(\frac{r_c^2}{2r_s B} \right)^2 - 1 + \xi_{\text{loss}} - \left(f_p \frac{L_p r_c^4}{2r_p^5} + f_s \frac{D r_c^4}{2r_s^5} + f_c \frac{z_0 - L_p + H}{2r_c} \right) \text{sign} \left(\frac{dH}{dt} \right) \right] \left(\frac{dH}{dt} \right)^2 \\
 & - g (H - h|_{r=r_D}) = 0
 \end{aligned}$$

The basic aquifer response (away from the well) is assumed to be Darcian and cylindrically convergent toward the well:

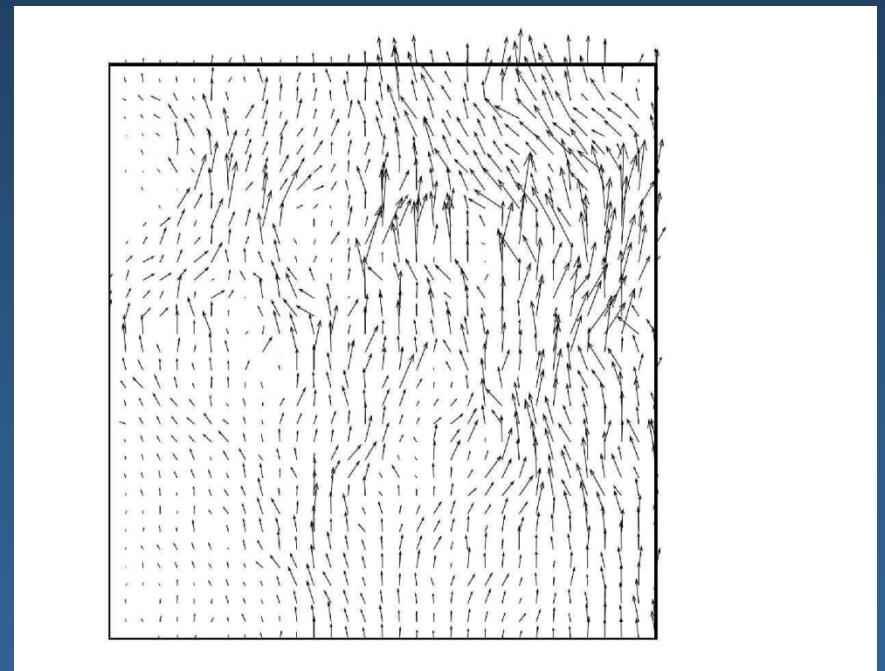
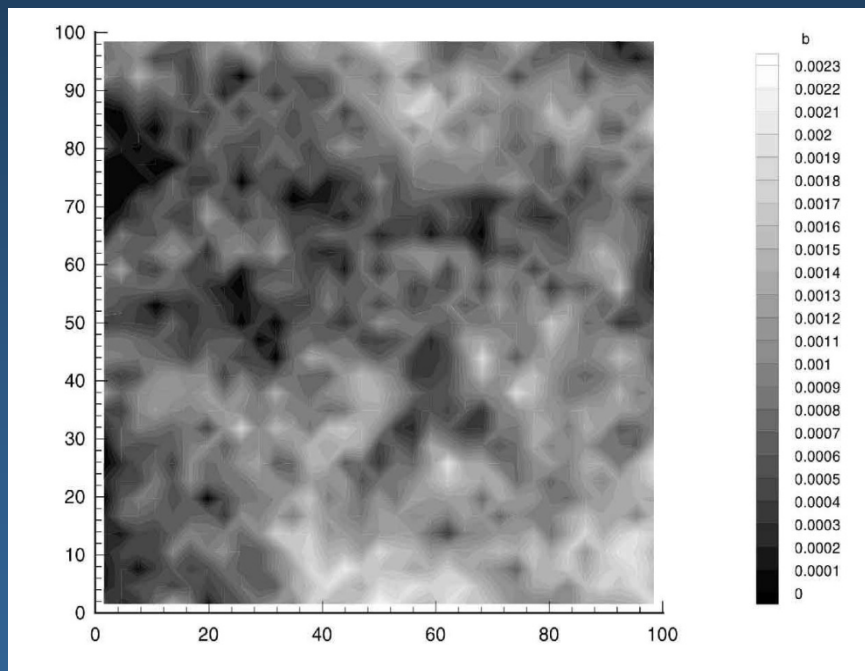
$$h|_{r=r_D} = -\frac{r_c^2}{2\pi^2 T} \int_0^t \frac{\partial^2 H}{\partial \tau^2} \int_0^\infty \frac{1 - e^{-\frac{4T(t-\tau)x^2}{Sr_D^2}}}{x^3 [J_1^2(2x) + Y_1^2(2x)]} dx d\tau$$

Note: The assumption of cylindrical flow convergence toward the tested well might not be correct for fractured rock settings in general. Any other (fractional) flow model could be used instead but a profound identification of the „true“ model governing formation flow might be difficult from slug testing alone.

Deviations from Darcian aquifer flow exist for:

- dominant electro-molecular forces (pre-linear laminar flow)
- dominant inertial effects due to flow path curvature, e.g. fracture flow channeling or flow in karstified rock (post-linear laminar flow)
- large flow rates in porous formations ($Re > 100$) resulting in turbulent flow (post-linear turbulent flow)
- significant fracture face roughness and sufficiently large flow rates ($Re > 2400$) resulting in turbulent fracture flow (post-linear turbulent flow)
- Non-Newtonian flow

Fracture flow channeling (from Kolditz, 2001):



Left: fracture roughness pattern (b = fracture aperture).

Right: simulated channelized velocity field.

Formation-related Nonlinearities:

A generalized rate-dependent skin effect is assumed to accommodate non-Darcian aquifer flow close to the well:

$$h\Big|_{r=r_D} - H_{\text{Filter}} = \pi r_c^2 \left(B_2 + C \left(\pi r_c^2 \right)^{p-1} \left| \frac{dH}{dt} \right|^{p-1} \right) \frac{dH}{dt}$$

Note: The above rate-dependent skin formula projects additional head losses associated with the nonlinearity of formation flow in an empirical manner onto the wellbore face. Therefore, one cannot tell from an application of the above formula how far into the formation nonlinear flow would be significant.

Wellbore-associated Nonlinearities:

Colebrook's formula is used to characterize turbulence inside the well:

$$\frac{1}{\sqrt{f_{p,s,c}}} = -2.0 \cdot \log_{10} \left[\frac{\varepsilon_{p,s,c}}{7.4r_{p,s,c}} + \frac{2.51}{\text{Re}_{p,s,c} \sqrt{f_{p,s,c}}} \right]$$

Backup: A new fully nonlinear slug test model

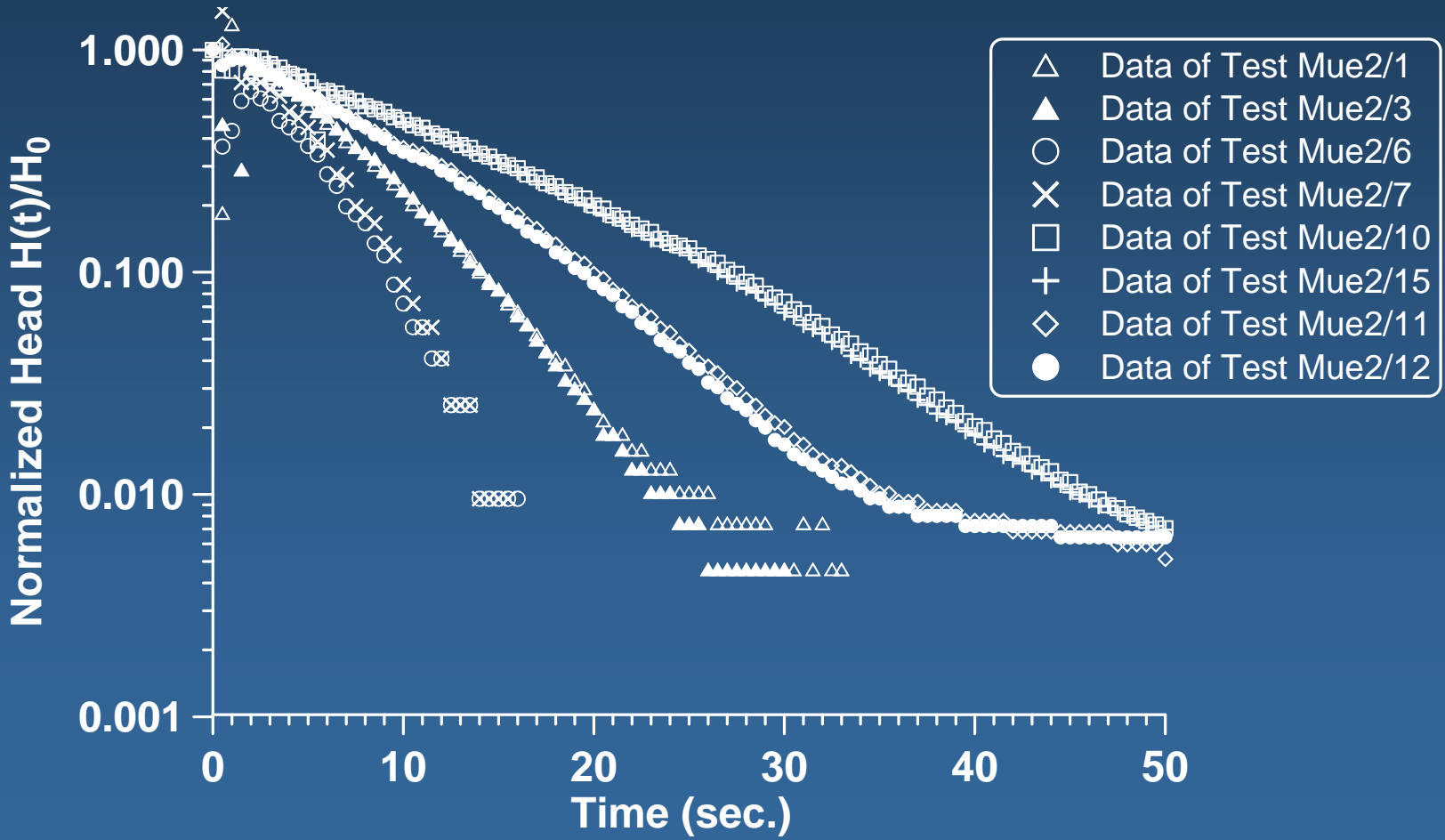
...and Borda Carnot-type head loss formulas to characterize minor head losses (shown here for the packer):

$$\left. \frac{\Delta p}{\rho} \right|_{\text{packer expansion}} = -\frac{1}{2} \left(1 - \frac{r_p^2}{r_c^2} \right)^2 \left(\frac{r_c^2}{r_p^2} \right)^2 \left| -\frac{dH}{dt} \right| \frac{dH}{dt} = -\frac{1}{2} \xi_{\text{packer-expansion}} \left| -\frac{dH}{dt} \right| \frac{dH}{dt}$$

$$\left. \frac{\Delta p}{\rho} \right|_{\text{packer contraction}} = -\frac{1}{2} \cdot 0.42 \left(1 - \frac{r_p^2}{r_c^2} \right) \left(\frac{r_c^2}{r_p^2} \right)^2 \left| -\frac{dH}{dt} \right| \frac{dH}{dt} = -\frac{1}{2} \xi_{\text{packer-contraction}} \left| -\frac{dH}{dt} \right| \frac{dH}{dt}$$

$$\xi_{\text{loss}} = -\left(\xi_{\text{packer-expansion}} + \xi_{\text{packer-contraction}} \right) \text{sign} \left(\frac{dH}{dt} \right)$$

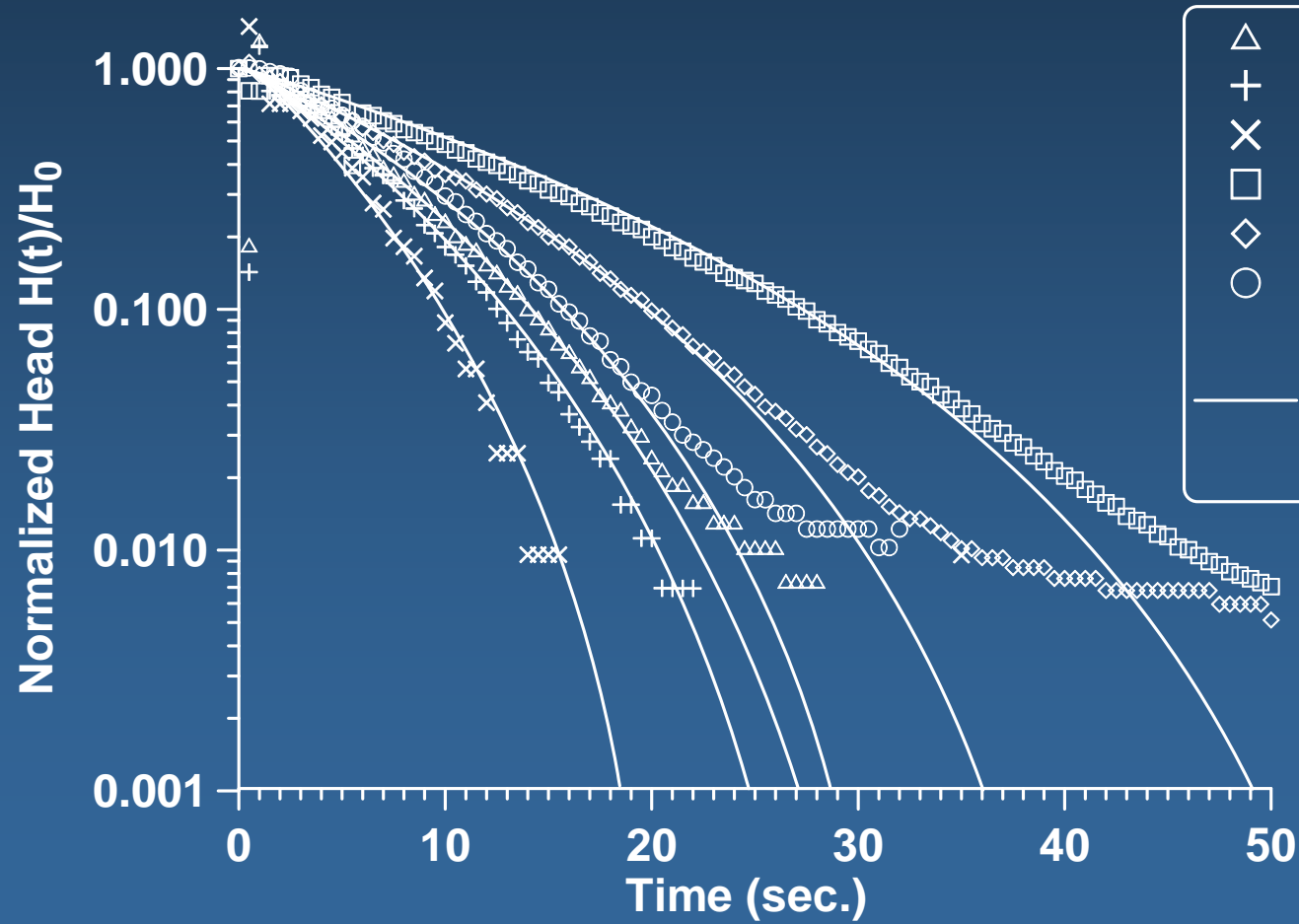
Data reproducibility: Repeated slug testing at well Münstereifelbohrung B2:



A Hvorslev-style variant of the nonlinear slug test model
(Zenner, 2006):

$$\begin{aligned}
 & - \left(H + z_0 + \left[\frac{r_c^2}{r_p^2} - 1 \right] L_p + \left[\frac{3}{8} B + D \right] \frac{r_c^2}{r_s^2} \right) \frac{d^2 H}{dt^2} - g \pi r_c^2 \left(B_2 + \frac{1}{F k_r} + C (\pi r_c^2)^{p-1} \left| \frac{dH}{dt} \right|^{p-1} \right) \frac{dH}{dt} \\
 & + \frac{1}{2} \left[\left(\frac{r_c^2}{2 r_s B} \right)^2 - 1 + \xi_{\text{loss}} - \left(f_p \frac{L_p r_c^4}{2 r_p^5} + f_s \frac{D r_c^4}{2 r_s^5} + f_c \frac{z_0 - L_p + H}{2 r_c} \right) \text{sign} \left(\frac{dH}{dt} \right) \right] \left(\frac{dH}{dt} \right)^2 \\
 & - g H = 0
 \end{aligned}$$

A Hvorslev-style variant of the nonlinear slug test model (Zenner, 2006):

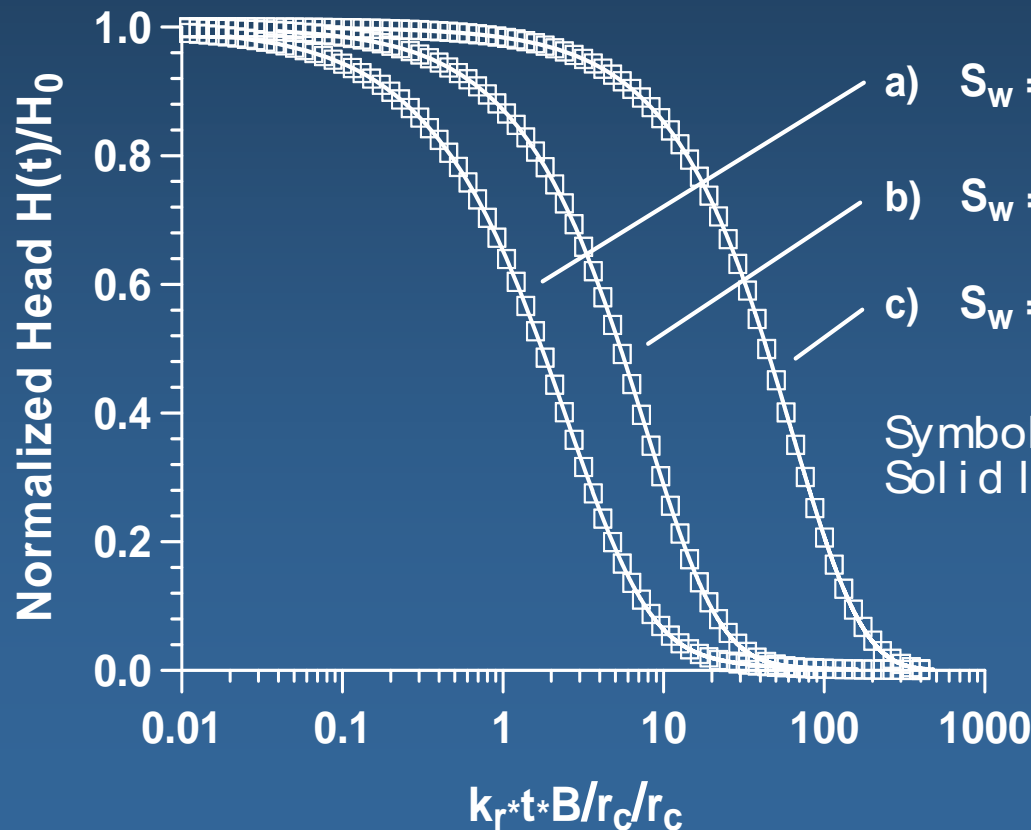


- \triangle Data of test Mue2/1
- $+$ Data of test Mue2/5
- \times Data of test Mue2/7
- \square Data of test Mue2/10
- \diamond Data of test Mue2/11
- \circ Data of test Mue2/14
- Simulations including all non-linear head losses but based on a Hvorslev-style variant of the nonlinear model

$k_f = 3.0 \cdot 10^{-4}$ m/s
 $C = 13000 \text{ sec.}^\rho / \text{m}^{3\rho-1}$
 $\rho = 1.5$
Hvorslev's case no. 7

Validation against the model of Dougherty & Babu (1984)
(fully penetrating case, with skin):

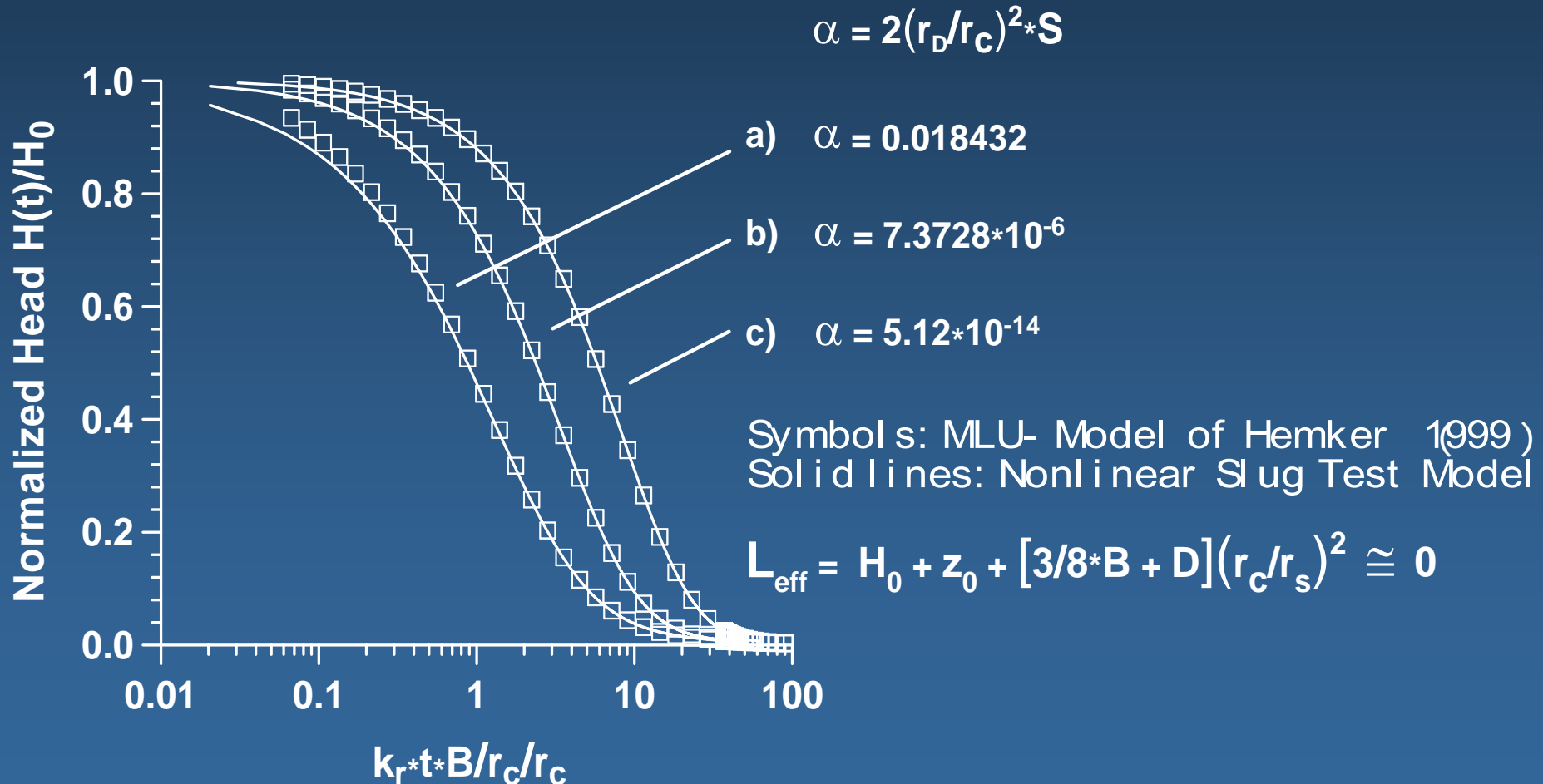
$$\alpha = 2(r_D/r_C)^2 * S = 0.0002$$



- a) $S_w = 0$ $B_2 = 0$
- b) $S_w = 10$ $B_2 = 3978.873577$
- c) $S_w = 120$ $B_2 = 47746.48293$

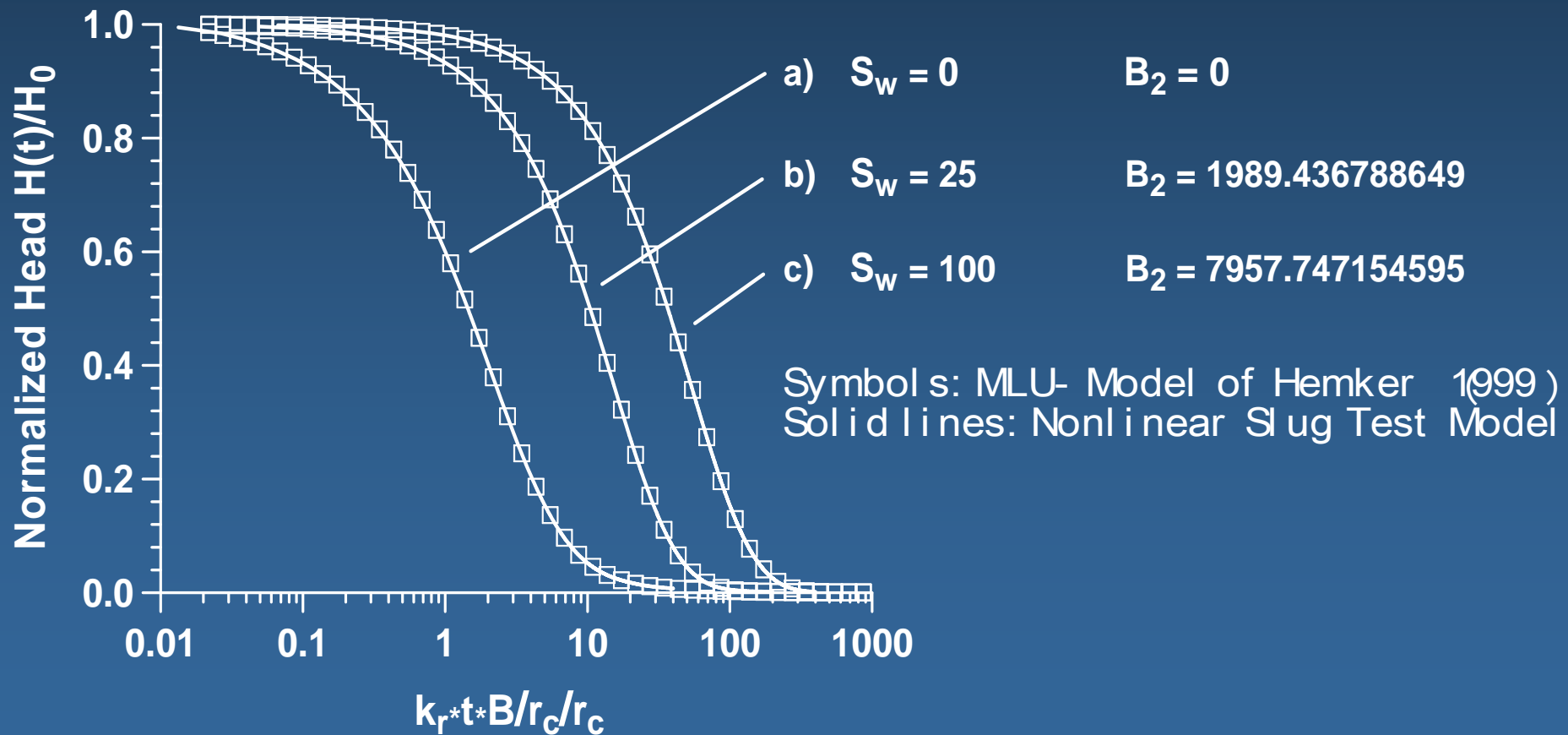
Symbols: Model of Dougherty & Babu (1984)
Solid lines: Nonlinear Slug Test Model

Validation against the MLU-model of Hemker (1999)
(one layer, no skin):



Validation against the MLU-model of Hemker (1999)
(one layer, with skin):

$$\alpha = 2(r_D/r_C)^2 * S = 0.001$$



References

- Barker, J.A. (1988). A generalized radial flow model for hydraulic tests in fractured rock, *Water Resources Research* 24(10), pp. 1796–1804.
- Cooper, H.H. Jr., J.D. Bredehoeft & I.S. Papadopoulos (1967). Response of a Finite Diameter Well to an Instantaneous Charge of Water, *Water Resources Research* 3(1), pp. 263–269.
- Dougherty, D.E. & D.K. Babu (1984). Flow to a partially penetrating well in a double-porosity reservoir, *Water Resources Research* 20(8), pp. 1116-1122.
- Hemker, C.J. (1999a). Transient well flow in vertically heterogeneous aquifers, *Journal of Hydrology* 225, pp. 1-18.
- Hemker, C.J. (1999b). Transient well flow in layered aquifer systems: the uniform well-face drawdown solution, *Journal of Hydrology* 225, pp. 19-44.

References (continued)

- Kolditz, O. (2001). Non-linear flow in fractured rock, International Journal of Numerical Methods for Heat & Fluid Flow 11(6), pp. 547-575
(<http://www.emeraldinsight.com/journals.htm?issn=0961-5539&volume=11&issue=6&articleid=877229>)
- Zenner, M.A. (2006). Zum Einfluss bohrlochinterner hydraulischer Verluste auf Wasserstandsreaktionen Packer-induzierter Auffülltests, Grundwasser 11(2), pp. 111-122.
- Zenner, M.A. (2008). Experimental Evidence of the Applicability of Colebrook and Borda Carnot-type Head Loss Formulas in Transient Slug Test Analysis, ASCE, Journal of Hydraulic Engineering 134(5), pp. 644–651.
- Zenner, M.A. (2009). Near-Well Nonlinear Flow Identified by Various Displacement Well Response Testing, Ground Water 47(4), pp. 526-535.

Acknowledgement

The presented work was supported in part by the German National Science Foundation (DFG) under Grant No. PE-362/24-2. The views and conclusions contained in this presentation are those of the author and do not necessarily reflect the official policies or positions, either expressed or implied, of the German Government.

The author wishes to express his gratitude to C.J. Hemker for providing his computer code MLU Version 2.2, with which part of the validation of the nonlinear slug test model was accomplished.